Supporting Information

FeS_2 intercalated montmorillonite as a multifunctional separator coating for high-performance lithium-sulfur batteries

Lian Wu,‡[a] Yifang Zhao,‡[a] Yue Yu, [a] Bing Liao,*[b] Hao Pang,*[a] and Haijiao Xie[c]

[a] Guangdong Provincial Key Laboratory of Industrial Surfactant, Institute of Chemical Engineering, Guangdong Academy of Sciences, Guangzhou 510665, Guangdong, P. R. China. E-mail: panghao@gdcri.com

[b] Guangdong Academy of Sciences, Guangzhou 510070, Guangdong, P. R. China. E-mail: liaobing@gic.ac.cn

[c] Hangzhou Yanqu Information Technology Co., Ltd., Hangzhou 310003, Zhejiang, P. R. China

‡ These authors contributed equally to this work

* **Corresponding author:**

Professor Hao Pang, Institute of Chemical Engineering, Guangdong Academy of Sciences, 318 Che Bei Xi Road, Tianhe District, Guangzhou 510665, China, E-mail: panghao@gdcri.com

Professor Bing Liao, Guangdong Academy of Sciences, 100 Xianlie Middle Road, Yuexiu District, Guangzhou 510070, China, E-mail: liaobing@gic.ac.cn

Contents

Additional experiment section

Determination of electrolyte uptake

The modified and unmodified separators were soaked in the electrolyte (1.0 M lithium bis(trifluoro-methanesulfonyl)imide (LiTFSI) and 2 wt% $LiNO_3$ in dimethoxyethane and dioxolane (DME/DOL) mixed solvent (1:1, v/v)) for 2 min. Excess amounts of the electrolyte droplets remaining on the separator surface were removed by scraping with a small brush. The electrolyte uptake (wt%) was calculated by the following equation (Eq. S1).

$$\textit{Electrolyte uptake}\ (\%) = (W - W_0)/W_0 \times 100\% \qquad \text{(Eq. S1)}$$

where W_0 and W is the weight of the separator before and after soaked in electrolyte, respectively.

Lithium-ion diffusion behavior characterization

(1) Lithium ions transference number

The modified/unmodified separators were separately sandwiched between two lithium metal electrodes in CR2025 coin cells with 30 μL Li-S battery electrolyte adding in each side of the separators. The lithium ions transference numbers of the separators were determined via the electrochemical combination method of direct current (DC) polarization and alternating current impedance.[1] Wherein, the DC polarization is the chronoamperometry at a constant step potential of 10 mV, and the EIS tests are conducted before and after DC polarization. The lithium ion transference numbers (t_{Li+}) are calculated via the following equation (Eq. S2).[1]

$$t_{Li+}=I_s(\Delta V\text{-}I_0R^0)/I_0(\Delta V\text{-}I_sR^s) \qquad \text{(Eq. S2)}$$

where ΔV is the applied voltage (10 mV), I_0 and I_s are the initial current and steady current, respectively, during DC polarization process. R^0, R^s are the charge-transfer resistances of Li symmetric cell before and after DC polarization, respectively.

(2) Ionic conductivity

The modified/unmodified separators were separately sandwiched between two stainless-steel electrodes in CR2025 coin cells with sufficient Li-S battery electrolyte. The ionic conductivities of the separators were determined by electrochemical impedance spectroscopy (EIS) from 100 kHz to 10 mHz with a potentiostatic amplitude of 5 mV and calculated by the following equation (Eq. S3).[2]

$$\sigma = \delta / (R_b \cdot A) \qquad \text{(Eq. S3)}$$

where σ is the ionic conductivity; δ is the thickness of the separator; R_b is the bulk resistance; A is the area of the stainless-steel electrode.

(3) Lithium-ion diffusion coefficient

CR2025 coin cells with the S/C cathodes, modified/unmodified separators, Li-S battery electrolyte, and lithium metal anodes were assembled. The lithium-ion diffusion coefficients of the separators were measured by performing a series of cyclic voltammograms (CV) tests at different scan rates and calculated according to the Randles-Sevick equation (Eq. S4).[3]

$$I_P = 2.69\times10^5 \cdot n^{3/2} \cdot A \cdot D_{Li}^{1/2} \cdot C_{Li} \cdot V^{1/2} \qquad \text{(Eq. S4)}$$

where I_P is the cathodic/anodic peak current; n is the charge transfer number (n = 2 for Li-S battery); A is the active electrode area (≈1.13 cm^2), D_{Li} is the Li ion diffusion coefficient; C_{Li} is the Li ion concentration in the electrolyte (10^{-3} mol·cm^{-3}); V is the scan rate.

Catalytic effect evaluation

The catalytic effect of the FeS_2@MMT composite on polysulfide conversion was tested by assembling CR2025-type symmetric cells with two identical electrodes, pristine PP separator and 40 μL Li_2S_6 electrolyte (0.5 M). The electrodes were made by coating the prepared FeS_2@MMT (or MMT) slurry on the aluminum foil. The areal mass loading was ~0.5 mg cm^{-2}. The Li_2S_6 electrolyte (0.5 M) was prepared by dissolving 230 mg Li_2S and 800 mg S in the 10 mL LiTFSI electrolyte. The CV curves were recorded in a voltage window of -1.5 to 1.5 V at a scan rate of 5, 10, and 15 mV s^{-1}. The EIS measurements were carried out in the frequency range of 10^{-1} to 10^5 Hz using with a perturbation amplitude of 5 mV.

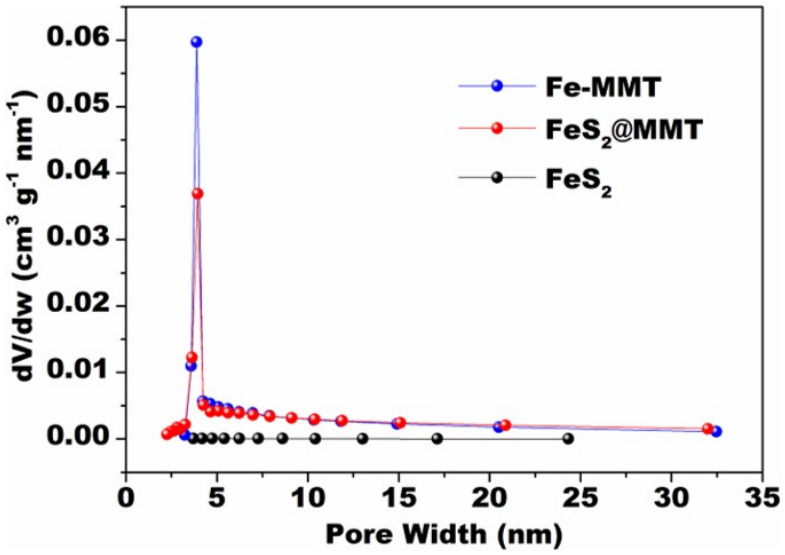

Fig. S1 Pore size distributions of FeS_2@MMT, FeS_2, and Fe-MMT.

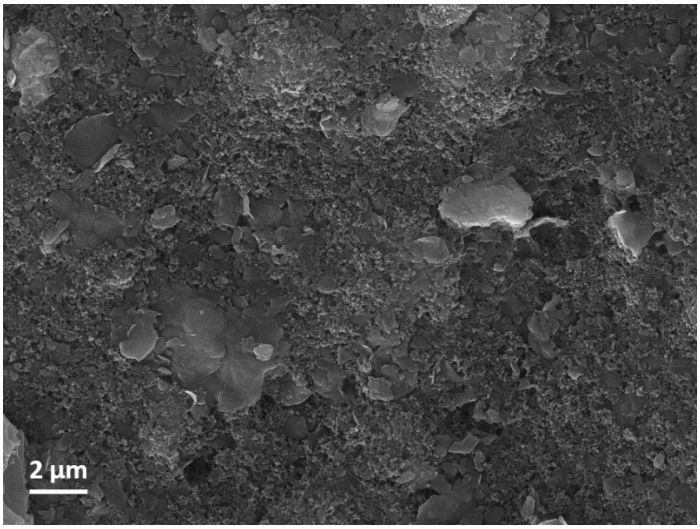

Fig. S2 SEM image of the surface of FeS_2@MMT coating layer.

Table S1 Pore structure characteristics obtained from conventional analysis of nitrogen isotherms.

Sample	S_{BET} (m^2 g^{-1})	Average pore diameter (nm)	Pore volume (cm^3 g^{-1})
Fe-MMT	83.3	7.3	0.29
FeS_2@MMT	65.7	9.7	0.24
FeS_2	0.8	36.8	0.002

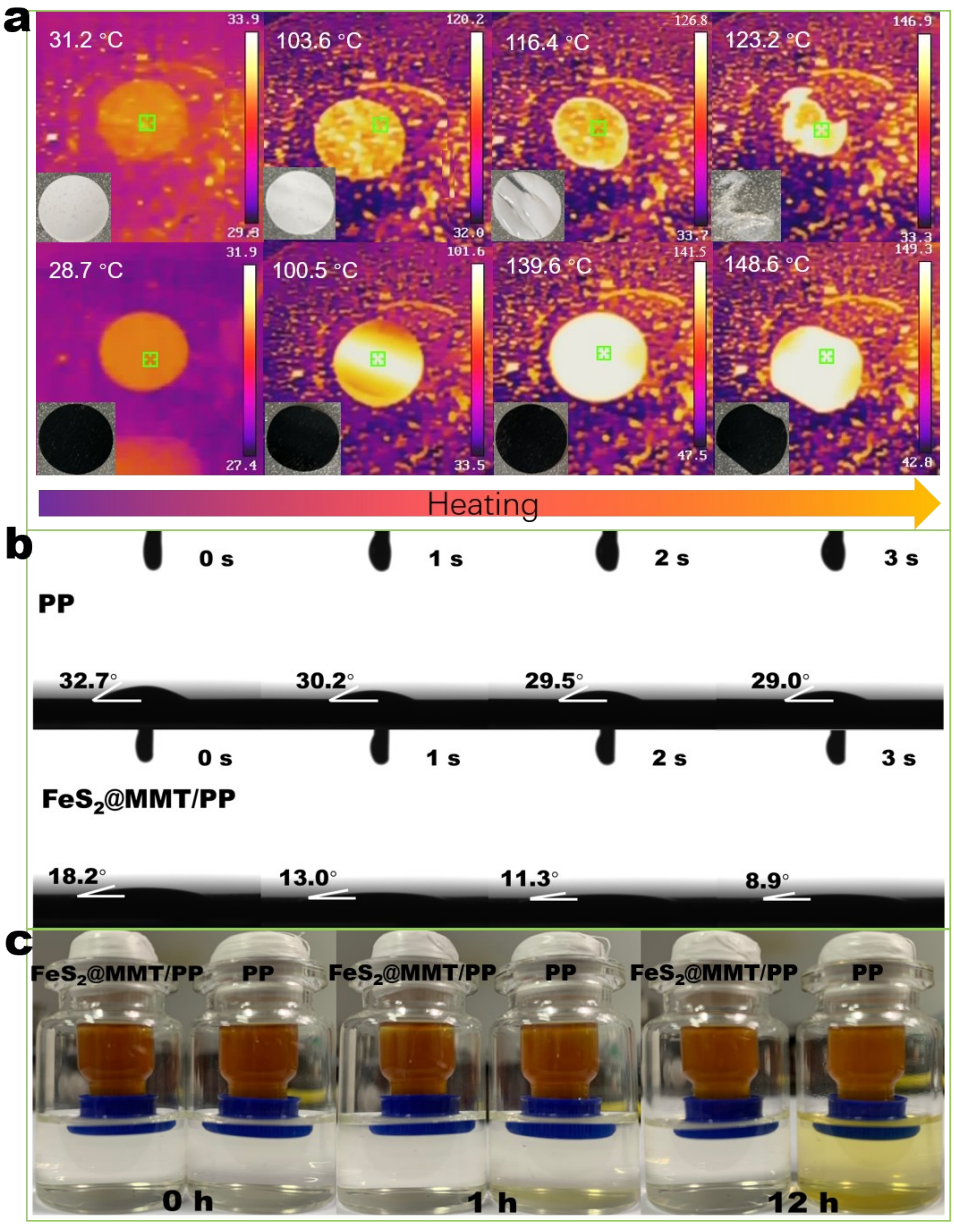

Fig. S3 (a) Infrared thermography images (from room temperature to 150 °C), (b) contact angles with electrolyte, and (c) polysulfide diffusion tests of the PP (Celgard 2400) and FeS2@MMT/PP separators.

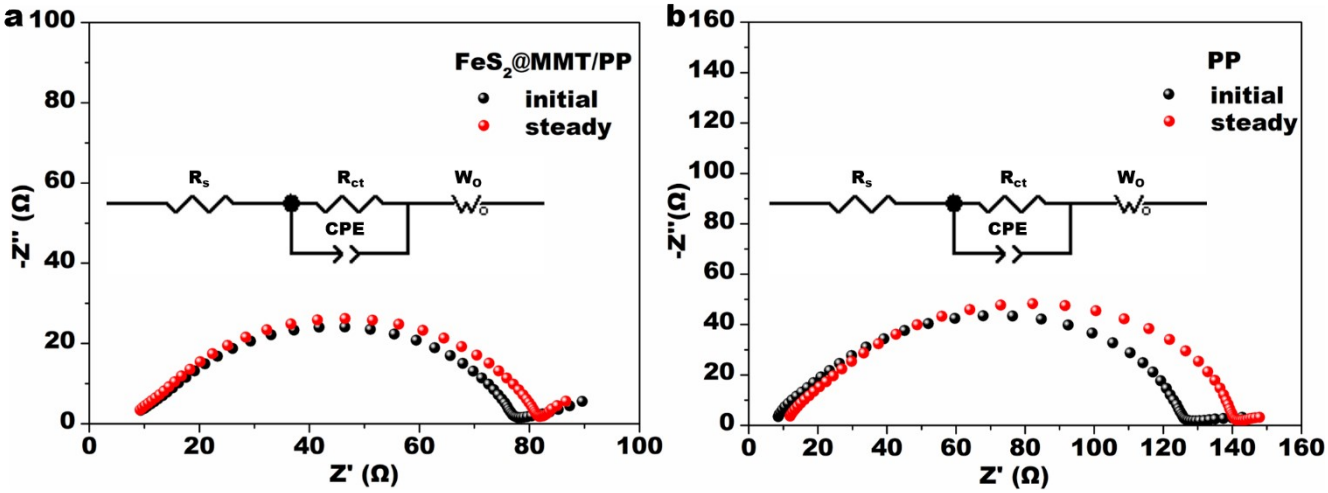

Fig. S4 AC impedance spectra and the corresponding simulating equivalent circuit of symmetrical battery with (a) FeS_2@MMT/PP and (b) PP separators.

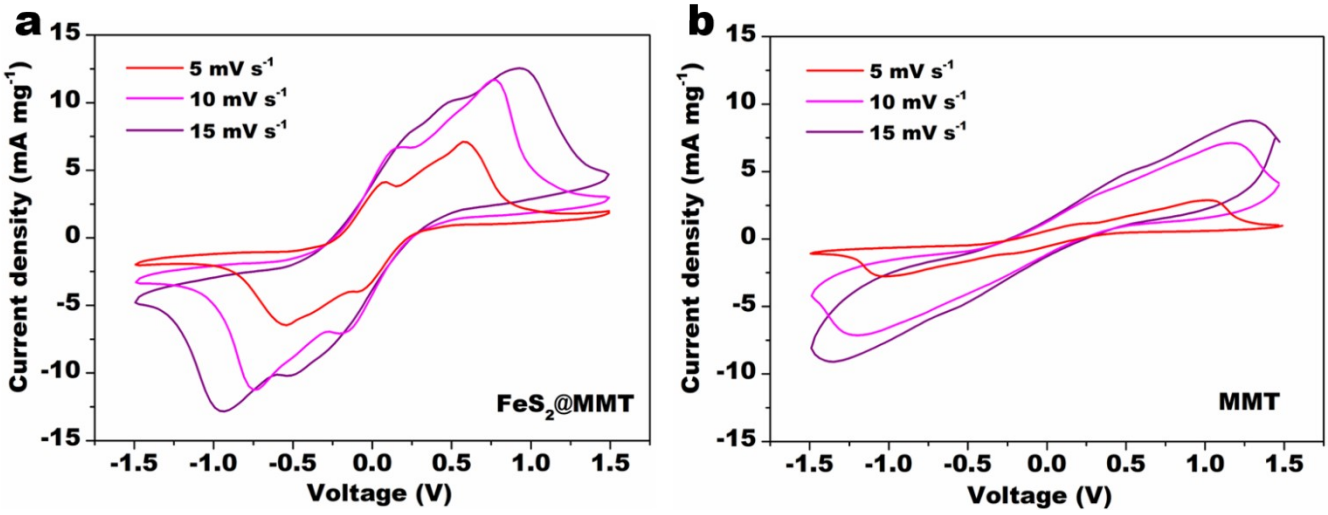

Fig. S5 CV curves of Li_2S_6 symmetric cells with with (a) FeS_2@MMT and (b) MMT electrodes at various scan rates from 5 mV s^{-1} to 15 mV s^{-1}.

Table S2 Values of R_s, R_{ct}, and W_C for various Li-S cells.

Separator used in the Li-S cell	R_s (Ω)	R_{ct} (Ω)	W_C (Ω)
FeS_2@MMT/PP	4.3	50.8	19.0
MMT/PP	10.5	75.3	21.3
Celgard 2400	3.5	66.1	28.5

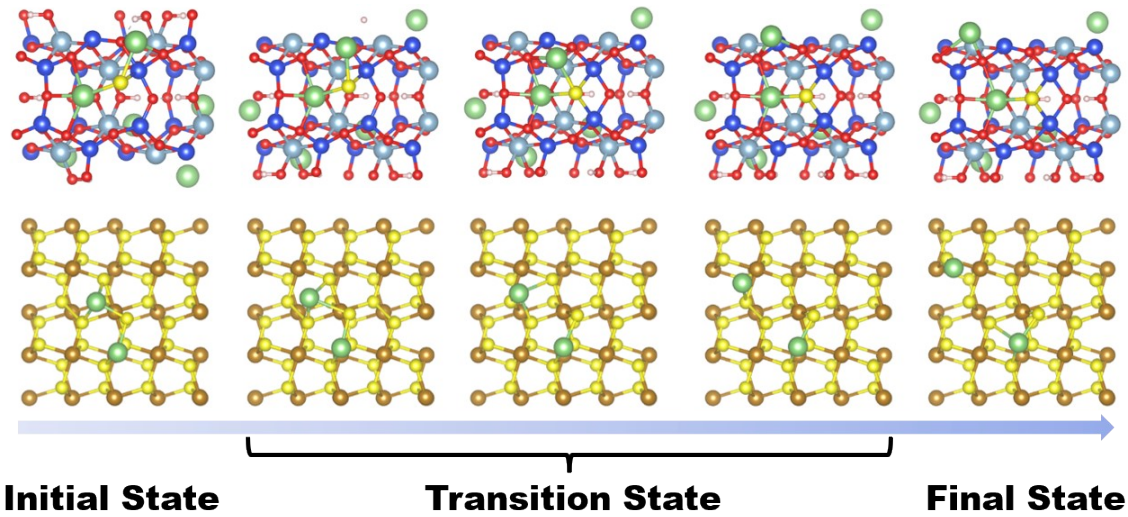

Fig. S6 Li_2S decomposition processes on MMT and FeS_2 (200) surface

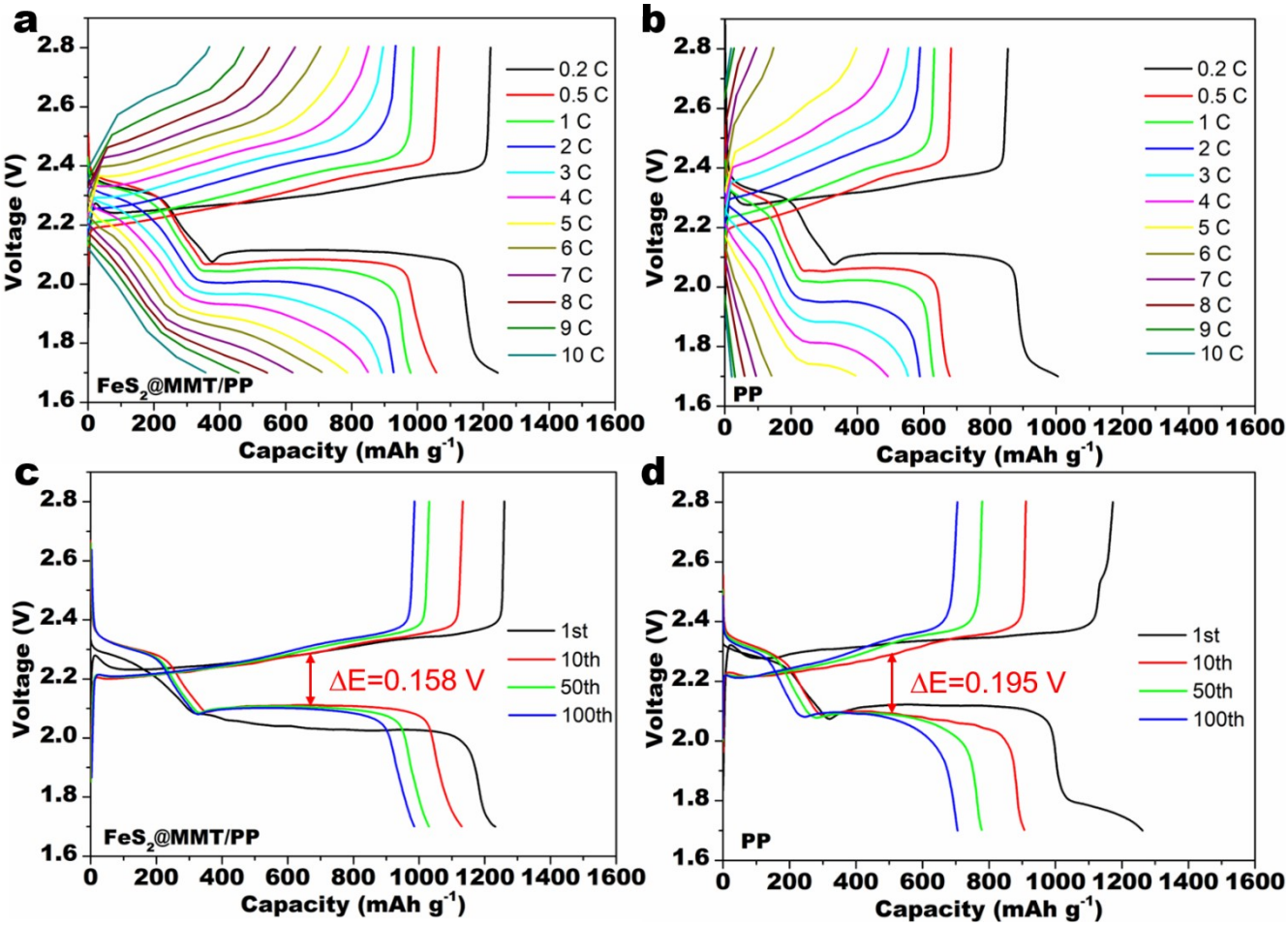

Fig. S7 Galvanostatic charge/discharge profiles of the cells with FeS_2@MMT/PP separator and Celgard 2400 separator at (a, b) various current rates and (c, d) at various cycles at 0.2 C.

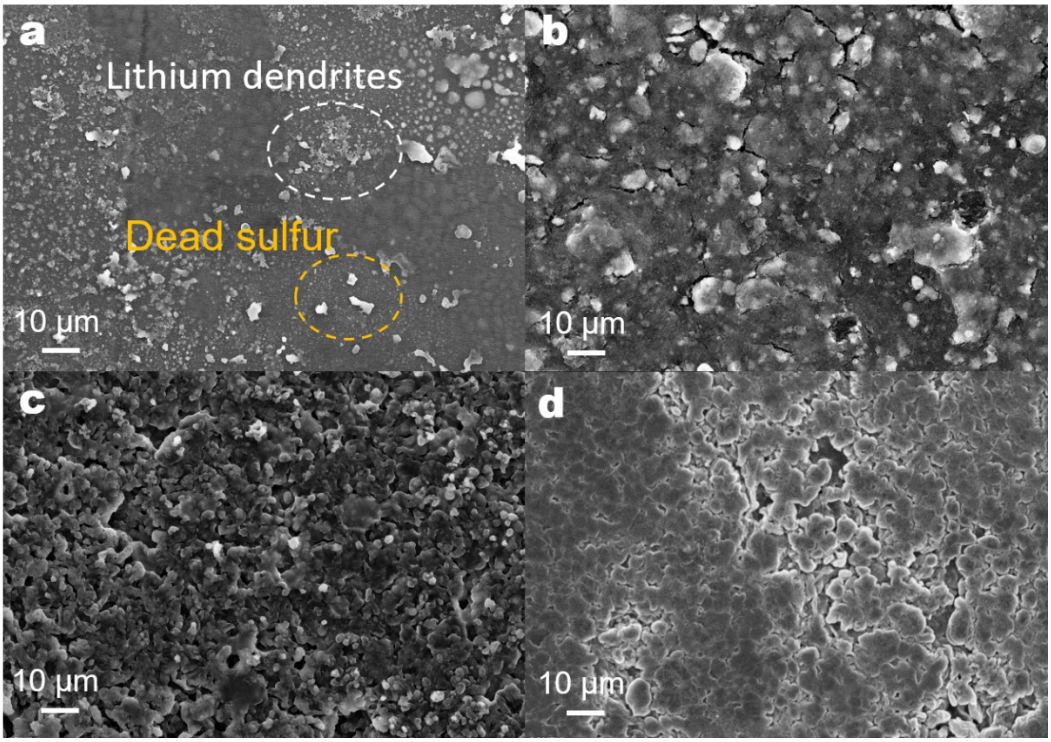

Fig. S8 SEM images of the (a) PP separator, (b) FeS_2@MMT/PP separator, (c) lithium anode in the cell with PP separator, and (d) lithium anode in the cell with the FeS_2@MMT/PP separator after 200 cycles at 0.2 C.

Table S3 Comparison of electrochemical performance between this work and previous works.

Coating layer	Cathode	Sulfur loading (mg cm^{-2})	Rate performance (C, mAh g^{-1})	Cycling performance			References
				Current rate (C)	Cycles	Reversible capacity (mAh g^{-1})	
$(PEI/MMT/PAA)_5$	KB/S	1.5	1 C, 335	0.5	200	560	[4]
MMT/RGO	MWCNT/S	1.5	3 C, 848	2	600	520	[5]
		5.71	/	0.1	40	770	
$Se_{0.06}$SPAN/MMT	BP2000/S	0.8	5 C, 669.9	1	1000	784.2	[6]
	MWCNT/S	6.96	/	0.1	60	849.1	
		26.75	/	0.005	20	1236.3	
PPY/Li-MMT	AB/S	1.0	3 C, 540	0.6	600	606	[7]
MMT@C	AB/S	2.6	0.7 C, 684	0.23	300	818	[8]
		4.5	/	0.25	90	700	
MMT	MWCNTs/S	0.7	/	0.06	200	924	[9]
Li-MMT	AB/S	1.5	/	0.2	190	776	[10]
MMT/CB	CNT/S	1.5	4 C, 379	1	500	666	[11]
		8.3	/	0.06	100	458	
FeS_2-NC	KB/S	1.6	2 C, 826.9	1	600	652.3	[12]
		5.0	/	0.5	100	715.6	
		7.1	/	0.5	100	459.5	
CoS_2@MMT	KB/S	1.0	7 C, 446	2	1000	676	[13]
		4.0	3 C, 595	0.2	100	853	
/	FeS_2/S	2.0	/	0.15	200	700	[14]
/	FeS_2/FeS/S	1.0	/	1	200	538.8	[15]
/	FeS_2-C/S	1.0	1 C, 750	0.5	350	761.2	[16]
/	$FeMoO_4/FeS_2/Mo_2S_3$ @S	2.3	10 C, 942	10	300	421	[17]
/	S/CPC@FeS_2	1.6	2 C, 916	1.5	900	540	[18]
		7.1	/	0.1	25	1239	
/	Li-MMT/S	1.2	2.5 C, 717	/	/	/	[19]
		2.0	/	1.5	600	600	
		5.2	/	0.92	350	480	
/	CoS_2@MMT/S	1.2	5 C, 548	2	500	519	[20]
		4.0	2 C, 577	0.2	200	630	
FeS_2@MMT	**KB/S**	**1.2**	**10 C, 358**	**0.2**	**200**	**940**	**This work**
				2	**1000**	**610**	
		5.0	**1 C, 400**	**0.5**	**200**	**564**	

References

[1] L. Chen, W. Li, L. Z. Fan, C. W. Nan and Q. Zhang, Intercalated electrolyte with high transference number for dendrite-free solid-state lithium batteries, *Adv. Funct. Mater.,* 2019, **29**, 1901047.

[2] S. Ruan, Z. Huang, W. Cai, C. Ma, X. Liu, J. Wang, W. Qiao and L. Ling, Enabling rapid polysulfide conversion kinetics by using functionalized carbon nanosheets as metal-free electrocatalysts in durable lithium-sulfur batteries, *Chem. Eng. J.*, 2020, **385**, 123840.

[3] X. Tao, J. Wang, C. Liu, H. Wang, H. Yao, G. Zheng, Z. W. Seh, Q. Cai, W. Li, G. Zhou, C. Zu and Y. Cui, Balancing surface adsorption and diffusion of lithium-polysulfides on nonconductive oxides for lithium-sulfur battery design, *Nat. Commun.*, 2016, **7**, 11203.

[4] A. Mentbayeva, S. Sukhishvili, M. Naizakarayev, N. Batyrgali, Z. Seitzhan and Z. Bakenov, Ultrathin clay-containing layer-by-layer separator coating enhances performance of lithium-sulfur batteries, *Electrochim. Acta*, 2021, **366**, 137454.

[5] X. Long, Z. H. Luo, W. H. Zhou, S. K. Zhu, Y. Song, H. Li, C. N. Geng, B. Shi, Z. Y. Han, G. M. Zhou, W. Lv and J. J. Shao, Two-dimensional montmorillonite-based heterostructure for high-rate and long-life lithium-sulfur batteries, *Energy Storage Mater.*, 2022, **52**, 120-129.

[6] W. Wang, K. Xi, B. Li, H. Li, S. Liu, J. Wang, H. Zhao, H. Li, A. M. Abdelkader, X. Gao and G. Li, A sustainable multipurpose separator directed against the shuttle effect of polysulfides for high-performance lithium-sulfur batteries, *Adv. Energy Mater.*, 2022, 2200160.

[7] M. Yang, J. Nan, W. Chen, A. Hu, H. Sun, Y. Chen and C. Wu, Interfacial engineering of polypropylene separator with outstanding high-temperature stability for highly safe and stable lithium-sulfur batteries, *Electrochem. Commun.*, 2021, **125**, 106971.

[8] M. Yang, Z. Li, W. Chen, Y. Hu and Y. Yan, Carbon-intercalated montmorillonite as efficient polysulfide mediator for enhancing the performance of lithium-sulfur batteries, *Energy Fuels*, 2020, **34**, 8947-8955.

[9] W. Ahn, S. N. Lim, D. U. Lee, K. B. Kim, Z. W. Chen and S. H. Yeon, Interaction mechanism between a functionalized protective layer and dissolved polysulfide for extended cycle life of lithium sulfur batteries, *J. Mater. Chem. A*, 2015, **3**, 9461-9467.

[10] M. Yang, N. Jue, Y. Chen and Y. Wang, Improving cyclability of lithium metal anode via constructing atomic interlamellar ion channel for lithium sulfur battery *Nanoscale Res. Lett.*, 2021, **16**, 52.

[11] W. Wang, Y. Yang, H. Luo and J. Zhang, Design of advanced separators for high performance Li-S batteries using natural minerals with 1D to 3D microstructures, J. Colloid Interf. Sci., 2022, 614, 593-602.

[12] Z. H. Liu, X. Mao, S. Wang, T. Li, Y. Luo, J. Xing, B. Fei, Z. Pan, Z. Q. Tian and P. K. Shen, A bifunctional interlayer fabricated by FeS_2-embedded N-doped carbon nanocages with efficient polysulfide trapping-catalyzing capability for robust Li-S batteries, *Chem. Eng. J.*, 2022, **447**, 137433.

[13] L. Wu, Y. Zhao, Y. Dai, S. Gao, B. Liao and H. Pang, CoS_2@montmorillonite as an efficient separator coating for high-performance lithium-sulfur batteries, *Inorg. Chem. Front.*, 2022, **9**, 3335-3347.

[14] S. S. Zhang and D. T. Tran, Pyrite FeS_2 as an efficient adsorbent of lithium polysulfide for improved lithium-sulphur batteries, *J. Mater. Chem. A*, 2016, **4**, 4371-4374.

[15] K. Xi, D. He, C. Harris, Y. Wang, C. Lai, H. Li, P. R. Coxon, S. Ding, C. Wang, and R. V. Kumar, Enhanced sulfur transformation by multifunctional FeS_2/FeS/S composites for high-volumetric capacity cathodes in lithium-sulfur batteries, *Adv.Sci.*, 2019, **6**, 1800815.

[16] D. Xie, S. Mei, Y. Xu, T. Quan, E. Härk, Z. Kochovski and Y. Lu, Efficient sulfur host based on yolk-shell iron oxide/sulfide-carbon nanospindles for lithium-sulfur batteries, *ChemSusChem*, 2021, **14**, 1404-1413.

[17] Z. Chen, A. Liao, Z. Guo, F. Yu, T. Mei, Z. Zhang, M. S. Irshad, C. Liu, L. Yu and X. Wang, A controllable flower-like $FeMoO_4/FeS_2/Mo_2S_3$ composite as efficient sulfur host for lithium-sulfur batteries, *Electrochim. Acta*, 2020, **353**, 136561.

[18] W. Sun, S. Liu, Y. Li, D. Wang, Q. Guo, X. Hong, K. Xie, Z. Ma, C. Zheng and S. Xiong, Monodispersed FeS_2 electrocatalyst anchored to nitrogen-doped carbon host for lithium-sulfur batteries, *Adv. Funct. Mater.*, 2022, 2205471.

[19] W. Chen, T. Lei, W. Lv, Y. Hu, Y. Yan, Y. Jiao, W. He, Z. Li, C. Yan and J. Xiong, Atomic interlamellar ion path in high sulfur content lithium-montmorillonite host enables high-rate and stable lithium-sulfur battery, *Adv. Mater.*, 2018, **30**, 1804084.

[20] L. Wu, Y. Yu, Y. Dai, Y. Zhao, W. Zeng, B. Liao and H. Pang, Multisize CoS_2 particles intercalated/coated-montmorillonite as efficient sulfur host for high-Performance lithium-sulfur batteries, *ChemSusChem*, 2022, **15**, e202101991.